

Application of double arrowhead auxetic honeycomb structure in displacement measurement

Zhengkai Zhang¹, Qingguo Wen^{1*}, Pengju Li¹, Hong Hu²

¹ School of Mechanical and Electrical Engineering, Xi'an University of Architecture and Technology, Xi'an, Shaanxi Province, P. R. China;

² Institute of Textiles and Clothing, The Hong Kong Polytechnic University, Hung Hom, Kowloon, Hong Kong, China

*Corresponding author, E-mail: wenqingguo@xauat.edu.cn

Abstract:

It is very important in measuring the amount of displacement in mechanical system and architectural structure. Researchers have developed displacement sensors using various materials and fabrication methods. In this study, a non-contact displacement measurement method based on the auxetic structure has been developed. By this method, the change of transmittance of the auxetic structure due to elastic deformation is transformed into the change of output current of the solar cell. The proposed method has potential applicability for measuring and monitoring of structural parts. The effectiveness of this method is investigated by geometrical analysis and experiments. This study provides new structural insights for displacement sensors and presents future research directions.

Key words: Auxetic structure, Displacement measurement method, non-contact measurement.

Introduction

Displacement measurement is very important in modern industry. All displacement sensors are made up of several components in common, including the actual sensing device, a transduction mechanism to convert the measurement signal to an electrical signal, and signal-processing electronics. They can be used to measure a whole range of measurands such as deformation, distortion, thermal expansion, vibration and so on. They have a wide range of application requirements in different fields, such as structural health monitoring [1], civil engineering [2]-[3], and manufacturing industries [4][5]. Many displacement measuring methods are relative in their operation, i.e. they can be contacting or non-contacting. However, most of displacement measuring methods are sensitive to environmental interference, high cost, and complex instrument adjustments. In addition, large volumes also make it difficult to integrate into an industrial system for automated online measurement. It is necessary to design and select the most appropriate measuring equipment according to cost, required accuracy, and usage environment.

In this paper, a simple non-contact way to measure the displacement is proposed. The measuring device consists of a light source, a solar cell and an auxetic structure. These three components are installed in a non-contact way. The principle of the measuring method is analyzed based on geometrical analysis. At the same time, a real auxetic structure is made and tested. Both the calculated and experimental results have verified the feasibility of the proposed method.

Analytical and numerical models

Auxetic structure

Auxetic materials and structures are those having negative Poisson's ratios. They transversally get fatter when stretched and thinner when compressed. Because of negative Poisson's ratio effect, the auxetic materials exhibit counter-intuitive behavior. Due to their unique structural features, they have been used in many applications, such as sports protection [6]-[7], medical Industry [8]-[9], sensors

[10]-[12] and actuators [13]. Auxetic mechanical metamaterials with their negative Poisson's ratio are used in stretchable strain sensors, and provide great sensitivity [14]. Interest on auxetic honeycombs lies upon the fact that auxetic materials with their negative Poisson's ratio are used in sensors, and provide great sensitivity [15].

Theoretical model

As shown in Fig.1, the unit cell geometry of 2D double arrowhead auxetic honeycomb structure has the following lengths across the x and y directions.

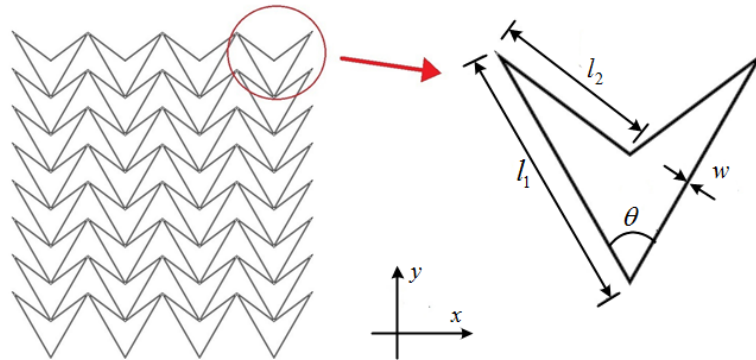


Fig.1. Layout of the unit cell

As shown in Fig.1, four parameters can define the cell geometry of a double arrowhead auxetic honeycomb cell, where θ denotes the internal angle between the two inclined cell ribs, l_1 and l_2 denote the length of two respective inclined cell ribs, and w is the cell wall thickness.

When the structure is compressed by force along the vertical direction, the angle θ will be decreased (see Fig.2). As a result, the structure contracts simultaneously in the horizontal and vertical directions.

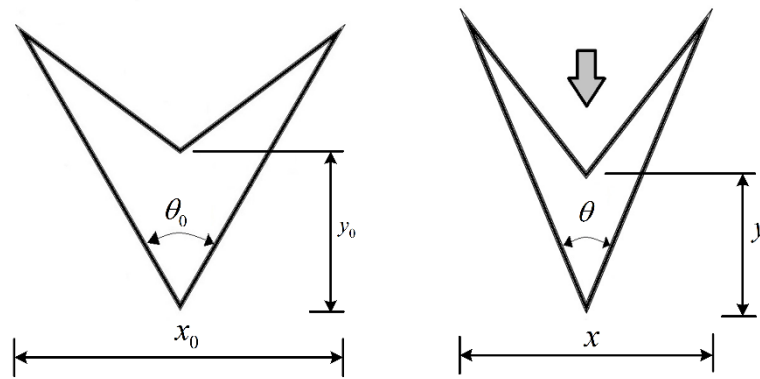


Fig.2. Resulting auxetic effects

Following the definition of Poisson's ratio one obtains [16]:

$$\nu_{yx} = -\frac{\varepsilon_y}{\varepsilon_x} = -\frac{\tan \theta \left(\frac{l_1}{l_2}\right) \sqrt{2(1 - \cos \theta) - \left(\frac{l_1}{l_2}\right)^2 (1 - \cos \theta)^2}}{1 - \left(\frac{l_1}{l_2}\right)^2 (1 - \cos \theta)} \quad (1)$$

The deformation of this geometry is depicted as shown in Fig. 2 and Fig. 3. It can be seen that the structure contracts in the horizontal direction when the force applied along the vertical direction.

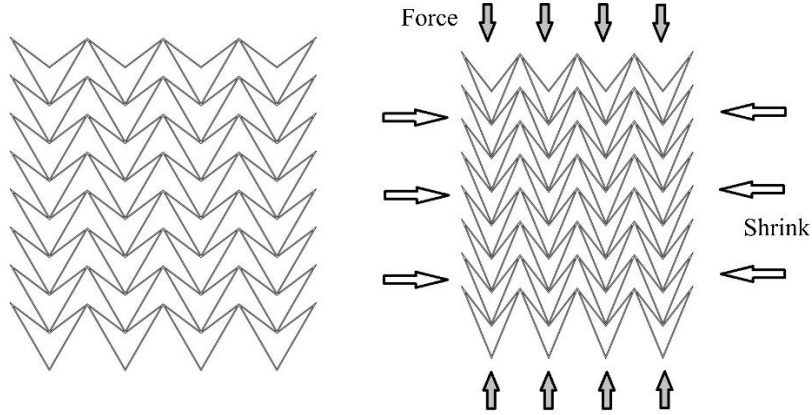


Fig.3. Deformation of the auxetic structure

As shown in Fig.4, when an auxetic structure placed parallel between a light source and a solar cell, a part of the light will be blocked by the auxetic honeycomb structure, and the other light will pass through the honeycomb structure and be received by the solar cell. The output current of the solar cell is depend on the amount of the light that received by it. When the auxetic structure is pressed longitudinally, it will shrink simultaneously in both the longitudinal and the lateral direction, as a result, more light will be blocked within unit area and the output current of the solar cell will be reduced accordingly. Based on this phenomenon, a correspondence can be established between the longitudinal shrinkage (may also be called displacement) and the output current of the solar cell.

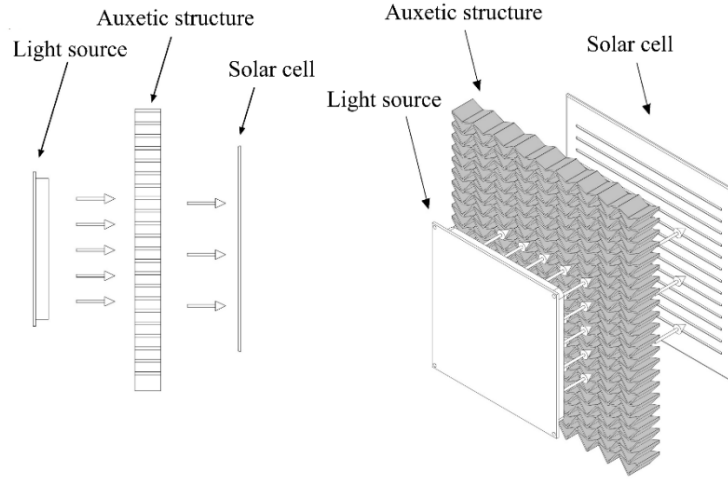


Fig.4. Principle of the proposed measuring method

The light-blocking area of an auxetic cell is:

$$S_{cell} = l_1 l_2 w \quad (2)$$

The area of an auxetic cell is:

$$S = \frac{l_1^2 \sin \theta}{2} - l_1 \sin \frac{\theta}{2} \sqrt{l_2^2 - l_1^2 \sin^2 \frac{\theta}{2}} \quad (3)$$

The porosity of the auxetic cell can be obtained by:

$$P = \frac{S - S_{cell}}{S} = \frac{\frac{l_1^2 \sin \theta}{2} - l_1 \sin \frac{\theta}{2} \sqrt{l_2^2 - l_1^2 \sin^2 \frac{\theta}{2}} - l_1 l_2 w}{\frac{l_1^2 \sin \theta}{2} - l_1 \sin \frac{\theta}{2} \sqrt{l_2^2 - l_1^2 \sin^2 \frac{\theta}{2}}} \quad (4)$$

Fig. 5 shows the variations of porosity with angle θ for given value of $l_1 = 5.2\text{mm}$, $l_2 = 3\text{mm}$ and $w = 0.5\text{mm}$. It can be seen that the porosity increases with the angle θ for a given value of l_1 , l_2 and w . Combined with Fig. 3 and Fig. 5, the porosity of the auxetic structure will decrease with the force increases.

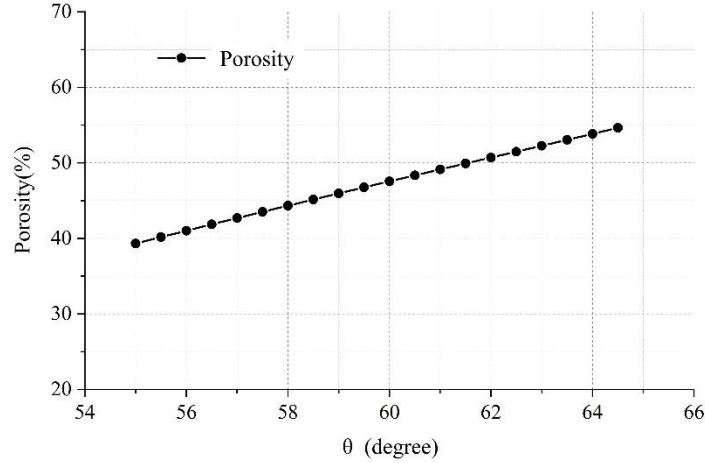


Fig.5. Variations of porosity with angle θ for given value of $l_1 = 5.2\text{mm}$, $l_2 = 3\text{mm}$ and $w = 0.5\text{mm}$

Experimental part

Specimen geometry

A large number of auxetic structures have been developed, the double arrowhead honeycomb structure is the one of the most common types, whose configuration is originally designed by Larsen [17]. The principle of this structure has been explained above. In order to further illustrate the role of auxetic structure in this measurement method, the hexagon honeycomb structure was used as a comparison in this experiment.

Fig. 6(a) and (b) show the two structure used in this study, the description of which are as follows:

- Double arrowhead honeycomb (Pattern A)

The double arrowhead honeycomb structure is characterized by the angle θ , cell strip length l_1 , l_2 and cell wall thicknesses w . In this study, Pattern A is formed using $\theta = 60^\circ$, $l_1 = 5.2\text{mm}$, $l_2 = 3\text{mm}$ and $w = 0.5\text{mm}$.

- Hexagon honeycomb (Pattern B)

The most common cellular honeycomb structure is periodically composed of perfectly regular cells. Within each hexagonal cell all six edges are of the same length l and all corner angles are equal to 120° . In this study, Pattern B is formed using $l = 6\text{mm}$ and cell wall thicknesses $w = 0.5\text{mm}$.

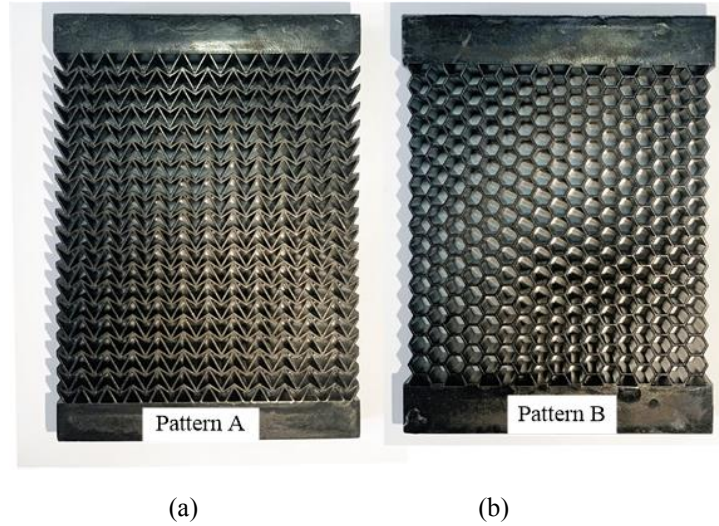


Fig.6. (a) Pattern A: $\theta=60^\circ$, $l_1=5.2\text{mm}$, $l_2=3\text{mm}$ and $w=0.5\text{mm}$. (b) Pattern B: $l=6\text{mm}$ and $w=0.5\text{mm}$.

Specimen preparation

The specimens were manufactured using 3D printed on an SLA printer (photo-sensitive polymer resin that hardens with UV light). The manufacturing principle of SLA 3D printer is using a high-powered laser to harden liquid resin that is contained in a reservoir to create the desired 3D shape. The physical properties of the material are summarized in Table 1. The accuracy of printing was approximately 0.025–0.05 mm and the production process took approximately 10 hours. In order to reduce the influence of reflection on the experiment results, the black resin of the specimens was painted black.

Table 1. Properties of the 3D printing material

| Properties of material | Value |
|------------------------|----------------------|
| Tensile modulus | 2.8GPa |
| Flexural modulus | 2.2GPa |
| Glass transition temp | 58.4°C |
| Poisson's ratio | 0.4 |
| Mass density | 1.2g/cm ³ |

Experimental set-up

The schematic diagram of the experimental set-up is shown in Fig.7. There is a 500K Ω resistor that connecting the solar cell in series. When the amount of light intensity on the solar cell changes, the current intensity generated by the solar cell will change accordingly, which resulting in a change in the voltage at both ends of the resistor. By measuring the change of the voltage at both ends of the cell, the intensity of light can be obtained.

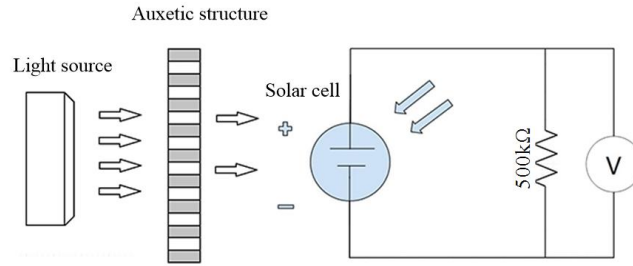


Fig. 7. Schematic diagram of the experimental set-up

The experiments were carried out using an in-house designed loading set-up based on a universal testing machine suitable for both optical measurement and displacement measurement. In order to avoid the interference of indoor lighting, the whole experimental apparatus is covered a dark box.

The light source used in this experiment is a plane light source, and the size of the luminous surface is 40mm×40mm. The light emitted by this source has an intensity of 360Lux at a distance of 20mm.

Solar cell is the basic unit of solar energy generation system where electrical energy is extracted directly from light energy. The solar cell produces electricity while light strikes on it and the voltage or potential difference established across the terminals of the cell is stabilize at a fixed value and it is nearly independent of intensity of incident light whereas the current capacity of cell is nearly proportional to the intensity of incident light as well as the area that exposed to the light. In view of the above characteristics of solar cell, we use a single crystal silicon solar cell with a size of 110mm×80 mm and working current 0-30mA (depending on light intensity) in this experiment.

The compression process was controlled by displacement. The maximum displacement was set to 2mm and the displacement is divided into 20 increments. During the test, the compression loads was applied on the upper face of the top plate and maintained at constant value, universal testing machine was employed to control the displacement. In order to prevent the sample tilt under large load, the load amplitude adopted in this experiment is relatively small (less than 800 N).

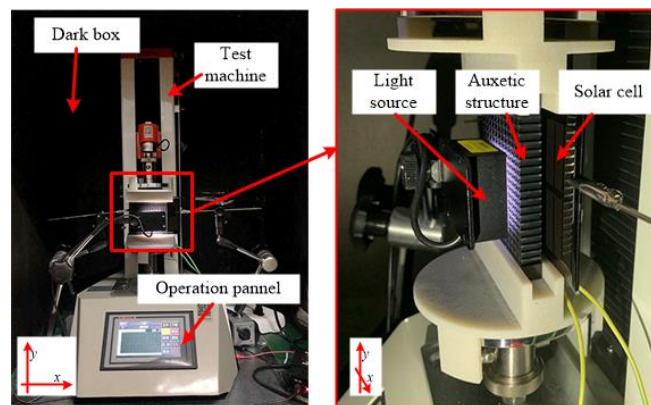


Fig.8. Auxetic structure sample mounted on the testing machine

Results and discussion

When there is no deformation, the output voltage in the initial state can be expressed as V_0 . When the auxetic structure is pressed, the structure will shrink in both horizontal and vertical directions, more light will be blocked within unit area and the output current of the solar cell will be reduced

accordingly. This leads to changes in the output voltage V_{output} . In this paper, we define the variation of voltage as ΔV .

$$\Delta V = |V_{output} - V_0| \quad (5)$$

In Fig. 9, the relationship between displacement and variation of voltage obtained by the proposed measurement method using two different honeycomb structures is plotted. In order to better study the nature of the relation between displacement and variation of voltage, line of best fit (Least Square Method) has also been plotted in the same figure. The slope of line of best fit characterizes the sensitivity of the proposed measuring method.

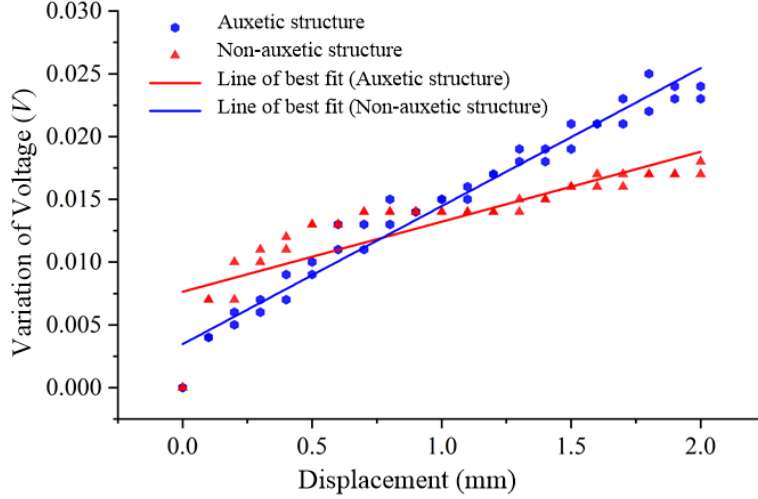


Fig.9. ΔV -displacement curves under maximum displacement of 2mm

As plotted in Fig. 9, the sample of the auxetic structure (Pattern A) with negative Poisson's ratio exhibited voltage change compared to the one with non-auxetic structure (Pattern B). The larger change in voltage indicates a higher sensitivity, which essentially validates the concept of this study. The sensitivity of the proposed measurement method based on two different structure was calculated and shown in Table 2. The sensitivity of the measurement method based on the auxetic structure is two times than that of the measurement method based on the non-auxetic structure.

Table 2. Sensitivity of Measurement Methods

| Measurement method | Sensitivity |
|-----------------------------|-------------|
| Auxetic structure based | 0.011mV/mm |
| Non-auxetic structure based | 0.0056mV/mm |

Moreover, this measurement method based on the auxetic structure still holds the original characteristics of high linearity. The linearity is not directly linked to the sensitivity but are important in displacement sensors, nonlinearity can make the calibration of the device more complex and difficult. The nonlinear errors is calculated with the deviation to line of best fit and referred to the nominal value and are shown in Table 3. The nonlinear error of the measurement method based on the auxetic structure is better than that of the measurement method based on the non-auxetic structure.

Table 3. Nonlinear Error of Measurement Methods

| Measurement method | Linearity | Full-scale | Nonlinear error |
|-----------------------------|-----------|------------|-----------------|
| Auxetic structure based | 0.00176V | 0.024V | 7.33% |
| Non-auxetic structure based | 0.00284V | 0.018V | 14.78% |

The measurement method based on the non-auxetic structure is inferior to that based on the auxetic structure in areas such as sensitivity and linearity. When the displacement continues to increase, the change of output voltage (ΔV) is not obvious. One of the leading factors is that the non-auxetic structure shrinks in the longitudinal direction after being compressed, but expands in the lateral direction, which results in the insignificant change in porosity.

To summarize, the deformation characteristics of the auxetic structure causes higher sensitivity and linearity in the proposed measurement method. The results validate the feasibility of the use of the auxetic structures for displacement measurement and thus contribute to further development.

Conclusion

In summary, this study demonstrates a fundamentally new non-contact way of measuring displacement. This method has been verified by building a simple measurement system, which has conclusively shown the correspondence between the input displacement and the output electrical signal. We note that there is a good linear relationship between the input and output of this measuring system, and shows good sensitivity and stability without using any signal processing means. These advantages are due to the special properties of the negative Poisson's ratio structure and are not found in hexagon honeycomb structures with positive Poisson's ratio.

It should also be noted that the three components (light source, auxetic structure and solar cell) of this measurement scheme are separate and do not have any physical connection with each other. This will undoubtedly make it more convenient in installation, as well as avoid interference and noise transmission.

Furthermore, this work provides not only a guide for the simple design of displacement measuring system but also serves as a basis for future investigations. The current design of the measuring method is only to validate the concept of this study and it can potentially be optimized for achieving better performance. Moreover, the proposed method also allows implementation of various auxetic geometries, which could further improve sensitivity of the measuring method proposed in this paper.

Acknowledgements

The research was supported by National Natural Science Foundation of China (No.51705394) and the Natural Science Basic Research Program of Shaanxi (No.2019JQ-758)

Reference:

- [1] Yang C, Oyadiji SO. Development of two-layer multiple transmitter fibre optic bundle displacement sensor and application in structural health monitoring, *Sens. Actuators A Phys.*, 2016, 244(15): 1-14. <https://doi.org/10.1016/j.sna.2016.03.012>.
- [2] Giri P, Kharkovsky S, Samali B. Inspection of metal and concrete specimens using imaging system with laser displacement sensor, *Electronics*, 2017, 6(2): 36. <http://dx.doi.org/10.3390/electronics6020036>
- [3] Giri P, Kharkovsky S. Dual-laser integrated microwave imaging system for nondestructive testing of construction materials and structures, *IEEE Trans. Instrum. Meas.*, 2018, 67(6): 1329-1337. <http://dx.doi.org/10.1109/TIM.2018.2795858>.
- [4] Lu M, Wang S, Bilgeri L. Online 3d displacement measurement using speckle interferometer with a single illumination-detection path, *Sensors*, 2018, 18(6):1923. <https://doi.org/10.3390/s18061923>.

- [5] Dong Z, Sun X, Chen C, Sun M. A fast and on-machine measuring system using the laser displacement sensor for the contour parameters of the drill pipe thread. *Sensors*, 2018, 18(4): 1192. <http://dx.doi.org/10.3390/s18041192>.
- [6] Toronjo A. Articles of apparel including auxetic materials. U.S. Patent: 20170099900A1, 13 April 2017.
- [7] Qiao JX, Chen CQ. Impact resistance of uniform and functionally graded auxetic double arrowhead honeycombs, *Int. J. Impact Eng.* 2015, 83: 47-58. <https://doi.org/10.1016/j.ijimpeng.2015.04.005>.
- [8] Ali MN, Busfield JJC, Rehman IU. Auxetic oesophageal stents: structure and mechanical properties, *J. Mater. Sci. Mater. Med.*, 2014, 25: 527-553. <https://doi.org/10.1007/s10856-013-5067-2>.
- [9] Kuribayashi K, Tsuchiya K, You Z, Tomus, D, Umemoto, M, Ito T, Sasaki M. Self-deployable origami stents as a biomedical application of Ni-rich TiNi shape memory alloy foil, *Mater. Sci. Eng. A*, 2006, 419: 131-137. <https://doi.org/10.1016/j.msea.2005.12.016>.
- [10] Jiang Y, Liu Z, Matsuhisa N, Qi D, Leow W R, Yang H, Yu J, Chen G, Liu Y, Wan, C. Auxetic mechanical metamaterials to enhance sensitivity of stretchable strain sensors. *Adv. Mater.* 2018, 30: e1706589. <https://doi.org/10.1002/adma.201706589>.
- [11] Ko J, Bhullar S, Cho Y, Lee PC, Martin B-G J. Design and fabrication of auxetic stretchable force sensor for hand rehabilitation. *Smart Mater. Struct.* 2015, 24: 75027. <https://doi.org/10.1088/0964-1726/24/7/075027>.
- [12] Jun S, Toshiaki N, Keita O. Sensitivity improvement of highly stretchable capacitive strain sensors by hierarchical auxetic structures. *Frontiers in Robotics and AI*, 2019, 6: 127. <http://dx.doi.org/10.3389/frobt.2019.00127>.
- [13] Lipton JI, MacCurdy R, Manchester Z, Chin L, Cellucci D, Rus D. Handedness in shearing auxetics creates rigid and compliant structures. *Science* 2018, 360: 632-635. <https://doi.org/10.1126/science.aar4586>.
- [14] Parth K, Hyun SK, Cho K-H, Joon YK. Cellular auxetic structures for mechanical metamaterials: a review. *Sensors* 2020, 20: 3132. <http://dx.doi.org/10.3390/s20113132>.
- [15] Ken EE, Andrew A. Auxetic materials: functional materials and structures from lateral thinking. *Adv Mater* 2000, 12(9): 617-628. [https://doi.org/10.1002/\(SICI\)1521-4095\(200005\)12:9<617::AID-ADMA617>3.0.CO;2-3](https://doi.org/10.1002/(SICI)1521-4095(200005)12:9<617::AID-ADMA617>3.0.CO;2-3).
- [16] Qiao JX, Chen CQ. Impact resistance of uniform and functionally graded auxetic double arrowhead honeycombs, *Int. J. Impact Eng.*, 2015, 83: 47-58. <https://doi.org/10.1016/j.ijimpeng.2015.04.005>.
- [17] Larsen UD, Sigmund O, Bouwstra S. Design and fabrication of compliant mechanisms and material structures with negative Poisson's ratio, *J. Microelectromech S*, 1997, 6(2): 99-106. <http://dx.doi.org/10.1109/84.585787>.

Declaration of interests

The authors declare that they have no known competing financial interests or personal relationships that could have appeared to influence the work reported in this paper.

The authors declare the following financial interests/personal relationships which may be considered as potential competing interests: